The American Journal of Pathology, Vol. 177, No. 4, October 2010

DOI: 10.2353/ajpath.2010.090063

Biomarkers, Genomics, Proteomics, and Gene Regulation

αB-Crystallin Is Elevated in Highly Infiltrative Apoptosis-Resistant Glioblastoma Cells

Dorota Goplen,*†‡ Sébastien Bougnaud,§ Uroš Rajcevic,§ Stig O. Bøe,* Kai O. Skaftnesmo,* Juergen Voges,¶ Per Ø. Enger,*‖ Jian Wang,* Berit B. Tysnes,* Ole D. Laerum,† Simone Niclou,§ and Rolf Bjerkvig*,§

From the Department of Biomedicine, and the Gade Institute,† University of Bergen, Bergen, Norway; the Departments of Oncology and Medical Physics,‡ and Neurosurgery,‖ Haukeland University Hospital, Bergen, Norway; the Departments of Neurology II and Stereotactic Neurosurgery,¶ Otto-von-Guericke-University Magdeburg and Leibniz-Institute for Neurobiology, Magdeburg, Germany; and NorLux Neuro Oncology Laboratory,§ CRP-Santé, Luxembourg, Luxembourg*

We have previously established two distinct glioma phenotypes by serial xenotransplantation of human glioblastoma (GBM) biopsies in nude rats. These tumors undergo a gradual transition from a highly invasive nonangiogenic to a less-invasive angiogenic phenotype. In a protein screen to identify molecular markers associated with the infiltrative phenotype, we identified α-basic-crystallin (αBc), a small heat-shock protein with cytoprotective properties. Its increased expression in the infiltrative phenotype was validated by immunohistochemistry and Western blots, confirming its identity to be tumor-derived and not from the host. Stereotactic human GBM biopsies taken from MRI-defined areas verified stronger αBc expression in the infiltrative edge compared to the tumor core. Cell migration assays and immunofluorescence staining showed αBc to be expressed by migrating cells *in vitro*. To determine αBc function, we altered its expression levels. αBc siRNA depletion caused a loss of migrating tumor cells from biopsy spheroids and delayed monolayer wound closure. In contrast, glioma cell migration in a Boyden chamber assay was unaffected by either αBc knockdown or overexpression, indicating that αBc is not functionally linked to the cell migration machinery. However, after siRNA αBc depletion, a significant sensitization of cells to various apoptotic inducers was observed (actinomycin, tumor necrosis factor α, and TNF-related apoptosis-inducing ligand [TRAIL]). In conclusion, αBc is overexpressed by highly migratory glioma cells where it plays a functional role in apoptosis resistance. ***(Am J Pathol 2010, 177:1618–1628; DOI: 10.2353/ajpath.2010.090063)***

Glioblastoma multiforme (GBM), the most common primary intracranial malignancy, is a morphologically diverse neoplasm with dismal prognosis despite multimodal therapy. At present, two-year survival of GBM patients with optimal therapy is less than 30%.[1] A major problem for effective glioma treatment is their highly invasive nature, where tumor cells can be identified several centimeters away from the main tumor mass. They are therefore incurable by local therapies such as surgery and radiotherapy.[2] Ninety-five percent of gliomas recur within 2.5 cm of the resection margin, which contains invasive cells that act as a "disease reservoir" and make current treatment options inefficient.[3] The mechanism of glioma cell invasion has been addressed in different studies and experimental settings, yet there is a need for novel markers characterizing the invasive phenotype.[4–6] The invasive phenotype is often poorly reflected in experimental model systems where GBM cell lines are xenotransplanted into the brain of immunodeficient animals. Generally, such tumors show a well-circumscribed growth with little single cell infiltration into the brain parenchyma.[5] To avoid this problem, we have developed a xenograft model where human brain tumor biopsy spheroids are transplanted into the nude rat brain.[7,8] The tumors derived from such spheroids show a highly infiltrative behavior in the central nervous system, reflecting the invasive characteristics of the human tumors *in situ* (low generation tumors). On serial transplantation *in vivo*, the

Supported by grants from the Norwegian Cancer Society, the Norwegian Research Council, CRP-Santé, Luxembourg, Helse Vest Haukeland University Hospital, and the sixth EU Framework Programme (Integrated Project "Angiotargeting", contract no. 504743 in the areas of "Life sciences, genomics, and biotechnology for health").

S.N. and R.B. contributed equally to this study.

Accepted for publication June 7, 2010.

Address reprint requests to Dorota Goplen, M.D., Ph.D., Department of Oncology and Medical Physics, Haukeland University Hospital, Jonas Lies vei 91, 5009 Bergen, Norway. E-mail: dorota@goplen.net.

tumors will develop a less invasive and more angiogenic phenotype (high-generation tumors).[9]

In a search of novel markers associated with the infiltrative phenotype, we performed comparative 2D protein electrophoresis of tumor samples obtained from low- versus high-generation tumors and identified several differentially expressed proteins. One of the proteins found to be highly expressed in the invasive phenotype compared to the less-invasive angiogenic phenotype was αB-crystallin (αBc), a small heat shock protein with chaperone and autokinase activity.[10–13] This protein is found in the central nervous system where it represents a major constituent of Rosenthal fibers (RF), which are intracytoplasmic inclusions frequently found within astrocytes in brain tissue of patients with Alexander disease.[14] αBc can associate with intermediate filaments and their soluble subunits such as vimentin and glial fibrillary acidic protein.[15–17] Previous studies have shown expression of αBc in astrocytic tumors, schwannomas, hemangioblastomas, chordomas, and renal cell carcinomas as well as in some glioma cell lines.[18,19] In the present study we show that αBc is mainly expressed by the infiltrative glioma cells both in experimental xenograft models as well as in human gliomas *in situ*. Moreover, we show that the molecule is not directly functionally linked to cell migration but plays a prominent role in apoptosis resistance.

Materials and Methods

Tumor Models and Cell Culture

Tumor fragments were obtained at surgery from GBM patients. Collection of tumor tissue was approved by the regional ethical committee at Haukeland University Hospital, Bergen, Norway. The specimens were collected from tumor areas appearing macroscopically viable, corresponding to regions with contrast enhancement on preoperative MRI scans. The specimens were transferred aseptically to test tubes containing a complete growth medium, which consisted of Dulbecco's modified Eagle's medium (DMEM) (Sigma-Aldrich, St. Louis, MO), supplemented with 10% FBS, 2% L-glutamine, 4× the prescribed concentration of nonessential amino acids, penicillin (100 IU/ml), and streptomycin (100 mg/ml).

Spheroids were prepared as previously described.[7] Briefly, tissue samples were minced into 0.5-mm-sized fragments and placed into 80-cm^2 tissue culture flasks (Nunc, Roskilde, Denmark) base coated with 10 ml of 0.75% agar (Difco, Detroit, MI) in DMEM. The spheroids were grown in a standard tissue culture incubator with 5% CO_2 in air and 100% relative humidity at 37°C, and the medium was changed once a week. After 1–2 weeks in culture, spheroids with diameters between 200 and 300 μm were selected for intracerebral implantation.

U-373MG human glioblastoma cells were cultured as monolayers in complete growth medium and passaged at confluence. Monolayers of cells were treated with trypsin-EDTA (BioWhittaker, Verviers, Belgium) as described before.[20] For the wound scratch and immunofluorescence experiments the cells were seeded in 24-well multidishes (Nunc), 10,000 cells per well.

Xenotransplantation Procedures

Nude rats (Han:rnu/rnu Rowett), 10 in each group, were fed a standard pellet diet and provided water *ad libitum*. All procedures were approved by The National Animal Research Authority. Biopsy spheroids were stereotactically implanted into the right brain hemisphere as described elsewhere.[21] Briefly, the animals were anesthetized by a subcutaneous injection of a mixture of midazolam, (Dormicum, Roche, Basel, Switzerland), 0.2 g per 100 g of body weight; fentanyl citrate, 0.0126 g per 100 g of body weight; and fluanizone, 0.4 g per 100 g of body weight (Hypnorm, Janssen, Oxford, United Kingdom). The rats were immobilized in a stereotactic frame (David Kopf Instruments, model 900, Tujunga, CA). After local anesthesia with Xylocain (AstraZeneca, Zug, Switzerland), a burr hole was made 3.0 mm to the right of the sagittal suture and 1 mm posterior to the bregma. Twenty-five microliters of PBS with 4.4 g/L glucose containing 10 spheroids was injected into the forebrain to a depth of 2.5 mm under the brain surface. Wound incisions were closed with 3.0 ethilon suture. Tumor growth was monitored at regular intervals during 4–20 weeks after implantation using a MRI Magnetom Vision Plus 1.5 T scanner (Siemens, Erlangen, Germany) and a small loop finger coil as previously described.[22,23] The animals were sacrificed by CO_2 inhalation when neurological signs were evident. The tumors were removed and new spheroids were generated, which again were transplanted into new animals. The animals that received the spheroids obtained from the patient tumor biopsy developed a highly invasive nonangiogenic phenotype after 4–6 months (low generation tumor). Gradually passaging of the tumors *in vivo* led to the development of a more angiogenic phenotype (high generation tumor; Figure 1A).[9,24] The brains were removed and fixed in 4% formaldehyde or snap frozen in liquid N_2 for further studies. In particular, coronal sections of tissue samples were macroscopically examined and solid tumor tissue was dissected out for further analysis. Previous acquired MRI images were used as a guide during dissection.

2D Protein Electrophoresis

For 2D electrophoresis, the tumor samples from four different cases were thawed, washed in Tris/sucrose solution (0.25 mol/L sucrose in 10 mmol/L Tris, pH 7.4) (Tris, Merck, Darmstadt, Germany; Sucrose, Sigma) and placed in sample buffer containing 7 mol/L urea, 2 mol/L thiourea (Merck), 4% CHAPS (Sigma), and 100 mmol/L dithiothreitol (DTT, Merck), and 1% pharmalyte (Amersham Biosciences, Uppsala, Sweden). The sample preparation was performed as described previously.[24] The protein concentration was estimated using the Bradford reagent (Bio-Rad, Hercules, CA). For the analytical gels, a protein load of 100 μg per gel was applied. The protein load for micro-

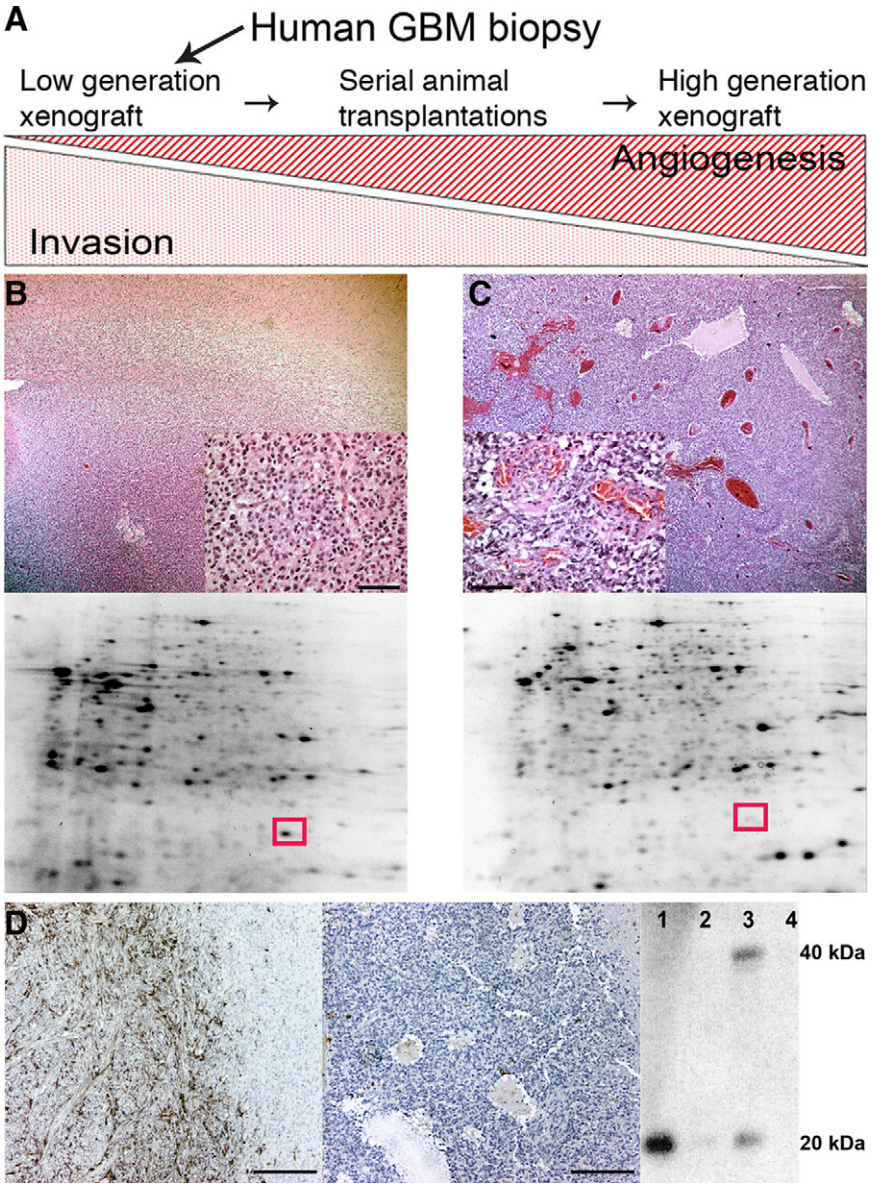

Figure 1. Differential expression of αBc in early and late-generation xenograft tumors established from human GBM in nude rats. **A:** Schematic illustration of the phenotypic shift from a highly invasive infiltrative phenotype (low-generation xenograft) to an angiogenic (high-generation xenograft). **B** and **C, top:** H&E-stained sections of low-generation and high-generation xenografts, respectively. **Inset:** High-power view of the tumor (Scale bar = 100 μm). **Bottom:** Corresponding protein 2D gel images of the tumors (**Red frame**: spot representing αBc). Please note: The 2D gels shown in **B** and **C** are the same as those used by Goplen et al,[24] with different spots highlighted. **D:** Verification of the differential expression of αBc by immunohistochemistry and Western blots. **Left:** Low-generation xenograft immunostained for αBc. **Middle:** High-generation tumor specimen immunostained for αBc. (Scale bars = 300 μm). **Right:** Western blots. Lanes 1 and 3, protein samples from low-generation tumors; lanes 2 and 4, tumor samples from the high-generation tumor samples. αBc expression can be detected both in dimer and tetramer forms.

preparative gels was 400 μg/gel. The 2D protein electrophoresis was performed as described previously.[24]

After the 2D electrophoresis, the analytical gels were silver stained, dried, and analyzed manually. Spots overexpressed in the invasive phenotype were selected. Thereafter, micropreparative gels with higher protein load were prepared and stained with SYPRO Ruby (Bio-Rad) immediately after the SDS-PAGE electrophoresis, according to the manufacturer's protocol. The gels were incubated in SYPRO Ruby overnight. The images of SYPRO Ruby stained gels were obtained by an image analyzer LAS-1000 (Fuji, Tokyo, Japan).

Mass Spectrometry

After manual excision, gel samples containing differentially expressed spots were stored at −80°C until further analysis. During the preparation of protein samples for mass spectrometry, the gel pieces were washed dried and in-gel trypsin digested (Promega, Madison, WI) overnight at 37°C. Thereafter, the peptides were extracted, lyophilized, reconstituted, and mixed with α-cyano-4-hydroxycinnamic acid (Promega) matrix solution directly on the MALDI target plate. Peptide mass spectra were generated on an Ultraflex MALDI-TOF (Bruker Daltonics, Bremen, Germany). The experimental peptide mass spectra was matched to the theoretical spectra using a peptide mass fingerprinting technique and a MASCOT search engine.[25] A probability based scoring was then obtained, showing a match between the experimental data and mass values calculated from candidate peptide sequences.

Immunohistochemistry

Immunostaining for αBc was performed on low- and high-generation tumors on tissue biopsies and on tissue microarrays. A high-density tissue microarray of primary

gliomas and normal human brain tissue (#GL208, U.S. Biomax, Inc, Rockville, MD) was used for immunohistochemical evaluation of αBc expression in a large number of samples. Tumor sections (5 μm thickness) of four grades were present in three replicates: Astrocytoma grade 1 (8 patients), astrocytoma grade 2 (22 patients) astrocytoma grade 3 (16 patients), and glioblastoma multiforme (15 patients), and 3 replicates (5 μm thickness) for each patient. Endogenous peroxidase activity was blocked with 0.03% hydrogen peroxide, and nonspecific binding was blocked with 2% fetal calf serum in 0.1% Triton X-100 Tris Buffered Saline (T-TBS, pH 7.6). The sections were then incubated for 1 hour at room temperature with a rabbit polyclonal anti- αBc (AB1546, Chemicon, Millipore, Billerica, MA) primary antibody. Immunohistochemical stainings were revealed using the HRPEnvision+ System HRP (anti-rabbit K4010, Dako). After washing, sections were incubated for 15 minutes with the DAB chromogen.

For quantification, all pictures were taken using the same background at a ×50 magnification on a Zeiss microscope. In total, 210 tissue spots were used for quantification: 27 cores from normal brain, 24 cores for Astrocytoma grade 1, 66 cores for astrocytoma grade 2, 48 cores for astrocytoma grade 3, and 45 cores for glioblastoma multiforme grade 4. Eight-bit pictures were analyzed with the Image J software. The rolling ball algorithm was used to subtract the background, and the mean pixel intensity was determined. The higher value of pixels (white) is 255, for each core the attenuation was calculated by the subtraction 255 minus the pixel mean. Values were visualized as box plots, and statistical analysis was done using the Mann–Whitney Wilcoxon rank test ($P \leq 0.05$).

Spatial Distribution of αBc in Human Gliomas

To determine the spatial distribution of αBc in human glioblastomas, immunostaining was also performed on stereotactic biopsies obtained from the tumor core and from the tumor periphery. Three patients were enrolled into the study prospectively according to the following inclusion criteria: (i) pathological lesion on MRI-images suggesting cerebral glioma; (ii) indication for stereotactic biopsy (localization (eg, deeply seated, eloquent brain areas), diffuse growth pattern, multiple lesions).[26] Excluded were cases that had experienced previous radiation therapy and/or chemotherapy. The biopsy material was only taken for study analysis if the radiological diagnosis of a cerebral glioma was confirmed later by histopathology. All patients gave their written informed consent before stereotactic biopsy. Nonstereotactic MRI was performed 2–3 days before surgery. Thin slice axial images (T1- and T2-weighted) were obtained using a 3.0 Tesla (Philips Gyroscan ACS, Eindhoven, Netherlands), a 1.5 Tesla (Philips Gyroscan ACS), or a 1.0 Tesla scanner (Philips Gyroscan T10NT). For surgery the patient's head was fixed in general anesthesia in a modified Riechert-Mundinger stereotactic head ring. After intravenous injection of contrast medium (Solutrast, Byk Gulden, Konstanz, Germany; dose: 1.5 g iopamidol/kg) a stereotactic cranial computed tomography (CCT) was performed (SOMATOM PLUS 40, Siemens, Erlangen, Germany) with 2-mm slice thickness, no interslice spacing, and 2-mm table increment. Following direct fiducially based transformation of CT-images into the stereotactic coordinate system, we integrated preoperative MR images using landmark-based image transformation. For image-based and computer-assisted 3D-stereotactic treatment planning we used special software (STP3, Stryker-Leibinger, Freiburg, Germany). The biopsy tract defined on MR images had to penetrate the supposed infiltration zone, active tumor tissue at the border of the lesion and the center of the tumor. Tissue samples were taken as serial biopsies starting at a point proximal to the defined target and going continuously forward in 5 or 6 mm steps. Intracerebral placement of the biopsy instrument (Backlund spiral needle, OD: 2.3 mm) was confirmed by stereotactic radiography (STX-XRAY) using X-ray tubes installed in the operating room. The stereotactic biopsies were frozen in liquid N_2. After thawing, they were fixed in 4% formalin and paraffin sections were prepared as described above. The sections were then immunostained and quantified for αBc as described above.

Western Blots

The tumor xenograft tissue was homogenized in buffer containing CHAPS, K_2HPO_4, KH_2PO_4, EDTA (Merck), and Protease Inhibitor Cocktail Complete (Roche Diagnostics, Manheim, Germany), centrifuged, and the supernatants were transferred into new tubes. The protein concentration was determined and SDS/PAGE electrophoresis was carried out on a 12.5% gel at 100V for 2 hours. Proteins were transferred onto a PVDF transfer membrane Hybond-P (Amersham). Expression of αBc was detected using an anti-αBc mouse monoclonal antibody (Stressgen Bioreagents) at a concentration of 1:1000. The images were obtained using an image analyzer LAS-1000 (Fuji).

Spheroid Migration Assay

To assess functional parameters related to αBc expression in multicellular GBM spheroids, 24 spheroids derived from the highly invasive rat xenograft tumors were placed in 24-well plates, one in each well, and overlaid with 0.5 ml medium. After 3 days, when the spheroids were attached to the plastic surface and the cells had begun to migrate, they were fixed, immunostained for αBc, and studied by fluorescence microscopy. The migrating cells were washed twice with medium without serum and subsequently transfected with siRNAs. The diameter of the spheroids and the area covered by migrating cells was measured daily both before and after transfection using an inverted phase contrast microscope with a micrometer scale in the ocular. Cell migration was calculated as the distance from the center of the spheroid to the population of migrating cells most distant from the spheroid minus spheroid radius at the time of seeding. The medium was renewed every second day.

Immunofluorescence

Migrating spheroid cells, U-373MG glioma cells (that have an endogenous expression of αBc) were fixed in 4% paraformaldehyde in PBS, permeabilized with Triton X-100 (Sigma) in PBS, and incubated with monoclonal antibodies to αBc (SPA222 Stressgen Bioreagents, Ann Arbor, MI) at a 1:100 dilution. Secondary goat anti-mouse conjugated to Alexa 555 (A-2122, Molecular Probes) or FITC-labeled antibodies (SouthernBiotech, Birmingham, AL) were applied to visualize αBc expression. The slides were mounted using DAPI containing mounting medium (Vectashield, Vector Laboratories, Burlingame, CA).

siRNA Transfection

siRNAs were obtained from Eurogentec (Liege, Belgium). The siRNA sequences were as follows: siRNA1; 5′ GGUGUUGGGAGAUGUGAUU dTdT 3′, siRNA2; 5′ AACAUGAAGAGCGCCAGGA dTdT 3′, siRNA3; 5′ AUACCGGAUCCCAGCUGAU dTdT 3′. Control siRNA (GL2) against fire fly Luciferase: 5′CUUACGCUGAGUACUUCGAdTdT3′ Biopsy spheroids and cultured U-373MG cells were transfected using Oligofectamine (Invitrogen, Carlsbad, CA) as previously described.[27]

Wound Scratch Assay

Wound scratch assays were performed in 24-well plates, and the scratch in the monolayer culture of U-373MG cells (that show a strong endogenous αBc expression) was made using the tip of a micropipette. For siRNA-transfected and control cells, the scratch was made 48 hours after transfection. After wound generation, the image of the wound was captured using a Nikon microscope every 24 hours until the entire surface of the well had been covered by migrating cells. The distance between the migrating cells on the edges of the wound was measured at different points chosen randomly. The value of the average wound size was calculated.

Overexpression of αBc in U87 Cells

To determine whether αBc is directly linked to cell migration, we stably transfected U87 glioma cells (do not show endogenous αBc expression) with αBc and studied their migratory potential in a wound scratch assay and in a Boyden chamber assay. αBc cDNA (a generous gift by Dr. Hidenori Ito, Institute for Developmental Research, Aichi Human Service Center, Aichi, Japan)[14] was cloned into a lentiviral transfer vector and αBc-expressing lentiviral particles were generated in 293T HEK cells using a three-plasmid system as previously described.[28] U87 glioma cells constitutively overexpressing αBc were generated (U87αBC) by infection of wild-type U87 cells with αBc-expressing lentiviral particles. Immunofluorescence staining was performed to confirm the overexpression.

Cell Migration Assays

Wild-type U87 and U87αBC were grown on tissue culture inserts (ThinCert, Greiner Bio One, Wemmel, Belgium) with 8-μm pore size (# 665638), allowing migration to the lower side of the membrane. For each cell line 10^5 cells were plated in duplicates in three different ThinCerts and deposited in a 12-well plate (#665180, Greiner Bio One). The same medium [DMEM containing 10% fetal calf serum (FCS) supplemented with 100 U/ml Pen/Strep, and 400 μmol/L Glutamax] was used in the insert and the well. After 48 hours of culture, cells were incubated for 4 hours with MTT (3-(4,5-Dimethylthiazol-2-yl)−2,5-diphenyltetrazolium-bromide) (M6494, Invitrogen, Merelbeke, Belgium) and dissolved in DMSO (D2438, Sigma, Bornem, Belgium). The optic density was measured at 560 nm, and the percentage of migrating cells was calculated. One well of each duplicate was used to measure the total number of cells (upper and lower part of membrane) and the second well to measure the cells that had migrated to the lower part of the membrane thus corrected for cell proliferation. The experiments were done in triplicate and repeated twice. Statistical significance of the data were evaluated with a *t*-test.

MTT Proliferation Assay

Proliferation was measured using the Vybrant MTT Proliferation Assay (V13154, Molecular Probes, Invitrogen, Merelbeke, Belgium) according to the manufacturer's instructions. In brief, 10,000 cells were plated and cultured for 72 hours, MTT was added for 2 hours, cells were solubilized in DMSO, and the formazan precipitate was measured at 540 nm.

Apoptosis Assay

U-373MG glioma cells were seeded in six-well multidishes, 10^5 cells per well on day −3. On day 0, at about 70 to 80% confluence, the cells were transfected with αBc siRNA according to manufacturer's instructions. The control cells were transfected with mock siRNA, siGL. The apoptosis was induced at day +3 by adding Actinomycin D (BioVision Research Products, Mountain View, CA) to the cells at a final concentration of 1:1000. The culture was terminated, and both the floating and the attached cells were harvested after 24 hours. Apoptosis was detected using an ApoDIRECT *in situ* DNA Fragmentation Assay Kit (BioVision) and quantified by flow cytometry. Briefly the cells were pelleted after 24 hours of treatment with Actinomycin D. The pellet was resuspended in 0.5 ml of PBS and fixed in 5 ml 1% (wt/vol) paraformaldehyde for 15 minutes on ice. After washing in PBS, the cells were stored in 70% ethanol, −20°C until staining. The staining was performed using the ApoDirect Assay Kit. Apoptotic cells showed green FITC staining over an orange-red PI counter staining. The flow cytometry was performed using a FACSCalibur flow cytometer (Becton Dickinson, San Diego, CA). The num-

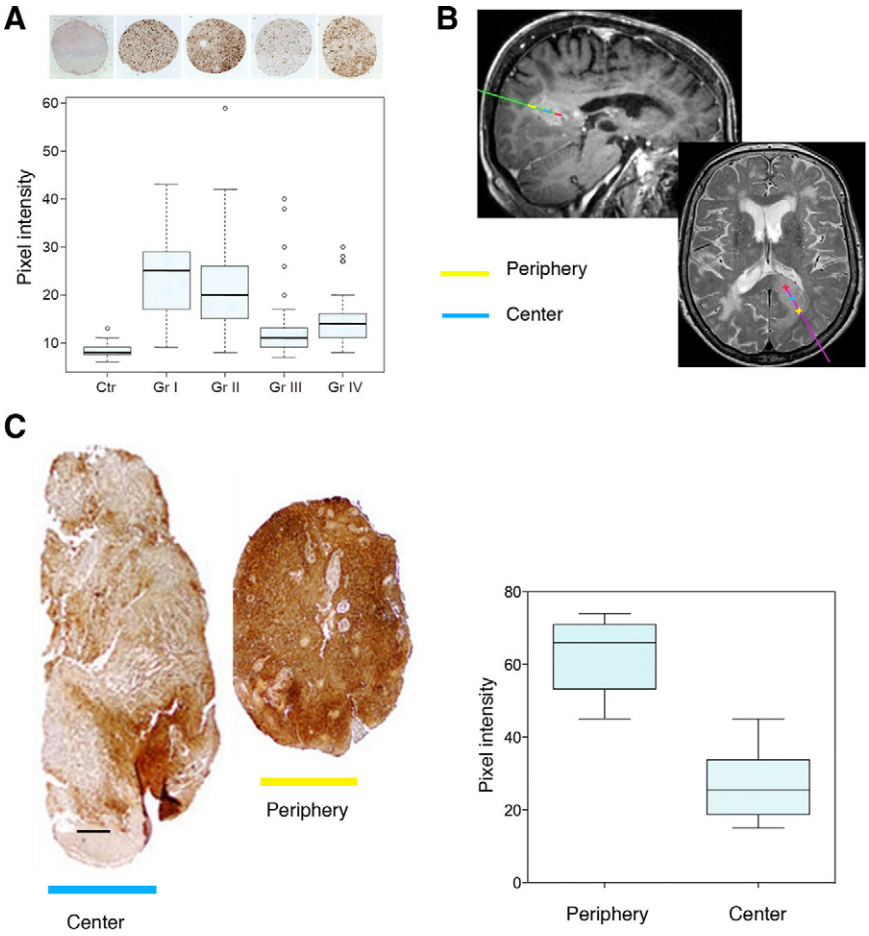

Figure 2. αBc immunohistochemistry of tissue microarrays of glioma grades I–IV. **A:** Quantification of immunostained tissue micraoarrays presenting normal brain (Ctr, 27 cores), astrocytoma grade I (Gr I, 24 cores), astrocytoma grade II (Gr II, 65 cores), astrocytoma grade III (Gr III, 39 cores), and glioblastoma multiforme (Gr IV, 47 cores). Quantification is represented as a box plot for all tissue samples analyzed. The difference between normal brain and all tumors as well as between low-grade (I and II) and high-grade gliomas (III and IV) is highly significant ($P < 0.001$). A representative immunostained tissue microarray sample is shown for each tissue sample on top of the graph. **B:** Stereotactic MRI-images from T1- and T2-weighted MR-sequences and sagittal and axial sections. The biopsy tract and location are color-coded. Colors on the sagittal section correspond to those indicated on the axial MRI images. On the axial section, the location of tissue sampling is indicated by a **cross**. **C:** αBc immunostaining of sterotactic GBM samples obtained from the center and periphery of the tumor. Included on the right is also a morphometric quantification of αBc expression. Scale bar = 100 μm.

bers of apoptotic cells in αBc siRNA-treated and in control samples were compared.

Apoptosis was also determined by using the cell apoptosis DAPI detection method. Briefly, 10,000 U-373MG cells were seeded into 24-well dishes (Nunc). After 24 hours the cells were treated with siRNA for 24 hours whereupon Actinomycin D (20 μmol/L), TNF-related apoptosis-inducing ligand (TRAIL; 50 ng/ml), tumor necrosis factor α (TNFα; 50 ng/ml) where added to the individual wells. Twenty-four hours after addition of the apoptotic inducers the nuclei where observed by fluorescence microscopy. Quantification of apoptotic cells where performed by counting 1000 cells in each well.

Results

Differential Protein Expression in the Invasive and Angiogenic Tumor Phenotypes

The tumor biopsies were taken from an area of contrast enhancement on MRI and were implanted into nude rat brains, as described before.[24] The experimental set-up and the generation of invasive and angiogenic tumor phenotypes obtained from serial passaging *in vivo* are shown in Figure 1, A–C, respectively. Comparative 2D-proteome analysis of these phenotypes revealed several differentially expressed proteins. All of the identified proteins were human. Among the identified proteins were structural proteins, stress-related proteins, brain-specific proteins, ECM proteins, and metabolic proteins. One of the identified proteins, up-regulated in low generation tumors with a significant score was αBc (CRYAB, Swiss Prot No: P02511, Figure 1, B and C). This protein was subsequently verified by immunohistochemistry and Western blots on brain tumor xenografts (Figure 1D). The data were also confirmed by a previous microarray analysis showing a 2.6-fold increased CRYAB gene expression in first generation infiltrative brain tumor phenotype.[9] By 2D proteome analysis αBc expression was also found to be increased in spheroids generated from GBM patient material compared to the biopsy material. Expression in spheroids was about 5 times higher than in the corresponding biopsy ($P < 0.001$, data not shown). This is of interest because the spheroids derived from the patient biopsy were used to generate the first generation (invasive) tumor in rats, which shows higher αBc expression than the late generation angiogenic tumors.

Expression of αBc in Low- and High-Grade Gliomas as Assessed by Tissue Microarrays

To determine whether αBc is expressed exclusively in GBM or whether its expression may also be detected in low-grade glioma we performed immunostaining of hu-

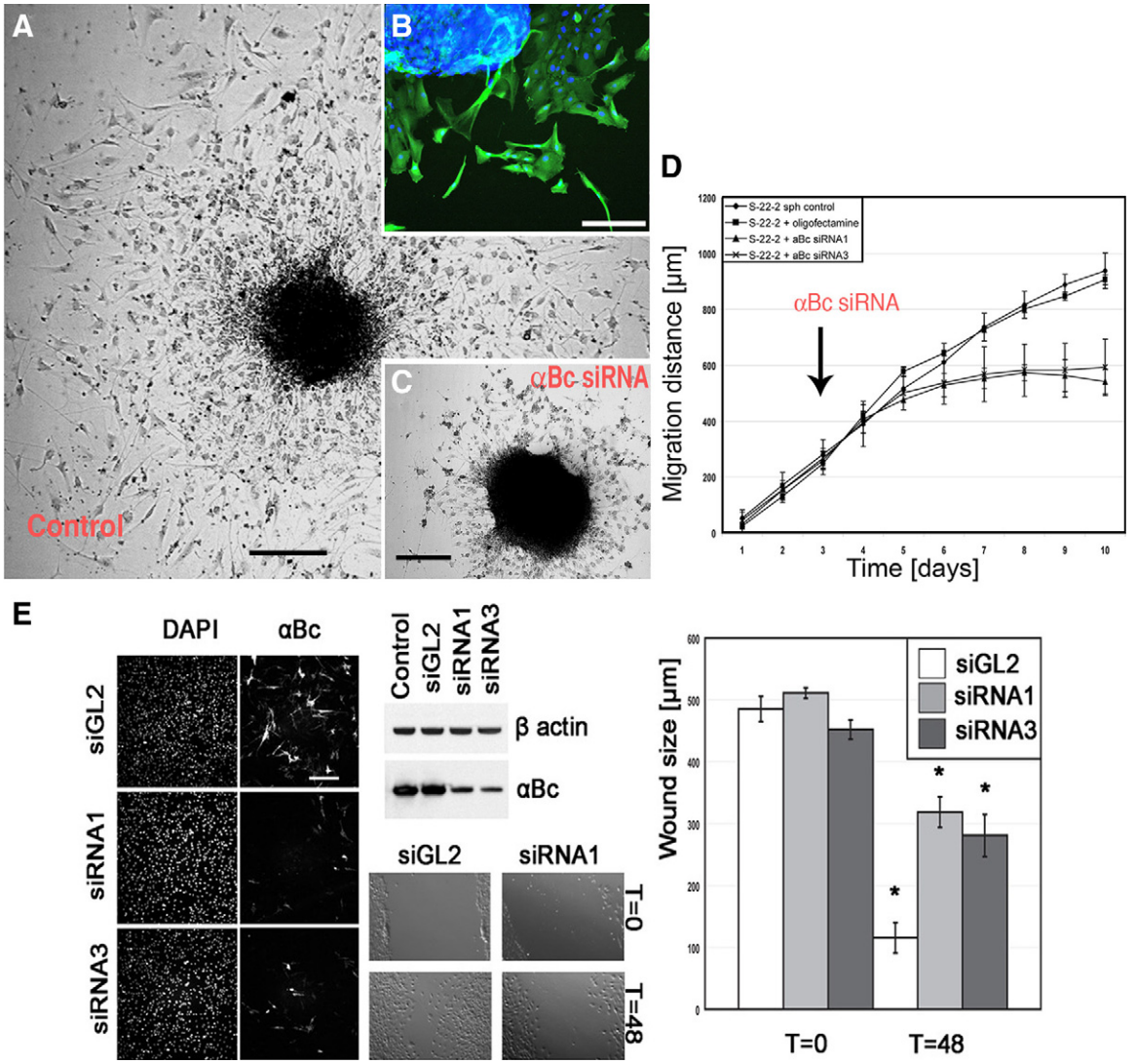

Figure 3. **A:** Cells migrating from GBM biopsy spheroids on a plastic surface (Scale bar = 100 μm). **B:** Immunostaining for αBc showing αBc-positive cells growing out from the spheroid. **C** and **D:** siRNA treatment led to a significant reduction of cells in the migration area compared to control cells (Scale bar = 100 μm; bars in **D** represents $\pm$ 1 SD). Sph, Spheroid. **E, left:** αBc immunostaining of U-373MG cells treated with siRNA shows a marked reduction in αBc expression (Scale bar = 100 μm). **Upper middle:** Immunostaining was verified by Western blots, showing reduced αBc expression in U-373MG cells after siRNA treatment; β actin is the control. **Lower middle:** Reduced number of cells in the wound closure area after siRNA treatment. **Right:** Quantification of wound closure after 48 hours of siRNA treatment (siGL2 represents control siRNA; $^*P < 0.05$).

man glioma tissue microarrays covering grade I—IV (Figure 2A). All four glioma types tested showed significantly higher αBc expression than normal human brain (Figure 2A; $P < 0.001$). Interestingly, αBc expression was strongest in grade 1 and grade 2 astrocytomas compared to high-grade gliomas (grade III and IV; Figure 2A). These data support the observations made in our animal models where the infiltrative phenotype show higher αBc expression compared to the more aggressive angiogenic phenotype which is known to have an extensive cell proliferation in the bulk tumor mass.[9] To further verify a connection between αBc and the infiltrative cellular component in gliomas, we assessed αBc expression in stereotactic biopsies that were carefully collected from MRI defined regions within GBMs, representing the infiltrative peripheral edge and the central tumor mass (Figure 2B). As shown in Figure 2C, αBc showed a stronger expression in the tumor periphery compared to the central tumor mass. This was observed for all tumors investigated (n = 3). Thus, our clinical observations support our experimental data in the animals (Figure 1D).

αBc Expression in Migrating Glioma Cells

Because cell migration is strongly associated with invasion and because αBc is overexpressed by highly infiltrative low generation tumor as well as in the invasive front of GBMs, we assessed the presence of αBc in migrating GBM cells derived from tumor biopsy spheroids (Figure 3, A and B). Immunofluorescence staining showed strong expression in cells that migrated out from the spheroid, whereas little staining was detected in cells that still remained within the spheroid (Figure 3B).

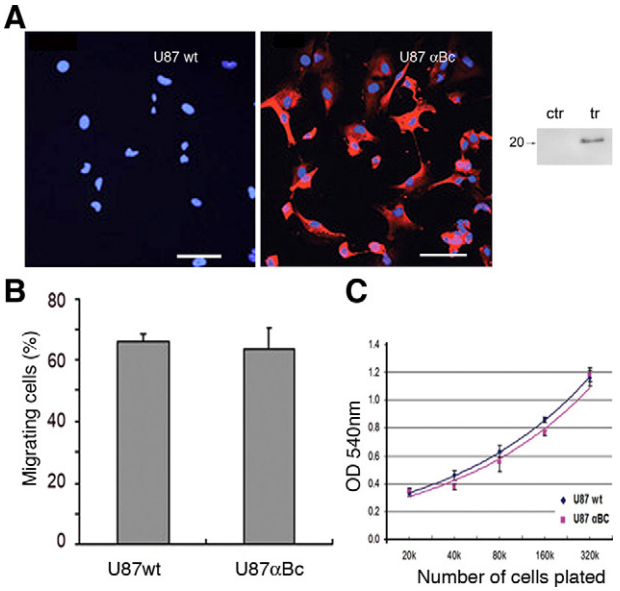

Figure 4. A, left: Immunostaining for αBc in wt U87 cells and U87 αBc-expressing cells (Scale bar = 30 μm); **Right:** Western blot obtained from control (ctr) and αBc-transfected (tr) cells. **B:** In a cell migration assay, no differences in migration were observed between the two cell populations. **C:** There were also no differences in cell proliferation between wt and U87 αBc-expressing cells.

We then treated the spheroid migration cultures with αBc siRNA. A strong reduction of migrating cells was seen from the spheroids after 48 hours, indicating that αBc knockdown affected the migrating cells (Figure 3, C and D). To further delineate the effect of siRNA on migrating tumor cells we transfected U-373MG cells, which show an endogenous expression of αBc, with siRNAs against αBc. At day three after transfection, αBc expression was strongly reduced compared to controls (Figure 3E). We then performed a wound-scratch assay, which determines the ability of cells to close a mechanically-induced lesion in a monolayer cell culture. As shown in Figure 3E, a delayed wound closure was observed in the αBc-depleted cells, also suggesting that loss of αBc affects the migrating cells.

Overexpression of αBc Does Not Increase Cell Migration

Because it is known that migrating glioma cells exhibit decreased levels of apoptosis,[29] we wanted to determine whether the αBc knockdown experiments affected the cell migration machinery or sensitized the migrating cells to apoptosis which also may account for the decreased number of cells observed in the migration experiments.

We overexpressed αBc in U87 glioma cells (which do not show endogenous expression of αBc) using lentiviral vectors (Figure 4A). Surprisingly the U87 αBc cells did not show increased migratory capability compared to the controls as no difference in the percentages of migrating cells were seen between U87 wild-type and U87 αBc cells after 24 and 48 hours of culture (Figure 4B). We also did not detect a difference in the proliferation rate between wild-type and U87 αBc expressing cells (Figure 4C).

Apoptosis Assay

To determine whether the delayed wound closure and reduced migration area might be due to an increased apoptosis and thus decreased cell number, we tested the relationship between αBc expression and induction of apoptosis in two independent apoptotic assays. Using a flow cytometry assay we exposed U-373MG cells and siRNA αBc-depleted cells to one dose of Actinomycin D. Figure 5A shows the difference between αBc-depleted cells treated with Actinomycin D and cells transfected with control siRNA and exposed to the same treatment. Transfection with αBc siRNA resulted in an increased sensitivity to apoptosis induction as shown by a higher percentage of apoptotic cells (21.6% for siRNA1-treated cells, 26.0% for siRNA3 vs. 10.7% for control cells). We also performed DAPI staining of U-373MG cells and U-373MG αBc-depleted cells treated with TNFα, TRAIL, and Actinomycin D (Figure 5B). Cell counts revealed a significant increase in apoptotic nuclei in the cells treated with siRNA (Figure 5C), showing that αBc has a significant role in apoptosis resistance.

Discussion

Malignant gliomas are associated with a dismal prognosis because of their infiltrative growth which prevents effective surgical resection.[29] Glioma invasion involves cell adhesion, motility, and remodeling of the ECM. It has been reported that certain ECM components, like vitronectin, preferentially expressed at the tumor-brain interface, confer a survival advantage of glioma cells by inducing expression of Bcl-2 and Bcl-X antiapoptotic proteins.[29,30] By proteomics and mass spectrometry we identified αBc to be associated with the invasive GBM phenotype.

αBc is known to be expressed in high-grade gliomas,[18,31,32] but little is known about its functional role in tumor progression. Genomic analyses of glioma cell lines exposed to motility inducing factors *in vitro* have been shown to up-regulate αBc transcripts.[33] In human breast carcinomas, αBc expression correlates with lymph node metastases, resulting in a poorer overall survival.[34] αBc levels also predict a poorer prognosis in basal-like breast carcinomas,[35] and a αBc expression can be down-regulated through BRMS1 (breast cancer metastasis suppressor gene), indicating an important role of this protein in tumor dissemination.[36] αBc has also been shown to protect cancer cells from TRAIL-induced apoptosis,[37] and vascular endothelial cells from glucose-induced apoptosis, indicating an antiapoptotic function.[38,39] In this context, αBc has been shown to antagonize caspase 3 activation by binding to a partially processed caspase 3.[38,40,41] αBc has also been shown to suppress differentiation-induced apoptosis and activation of caspase 3 in myoblasts during myogenesis.[42]

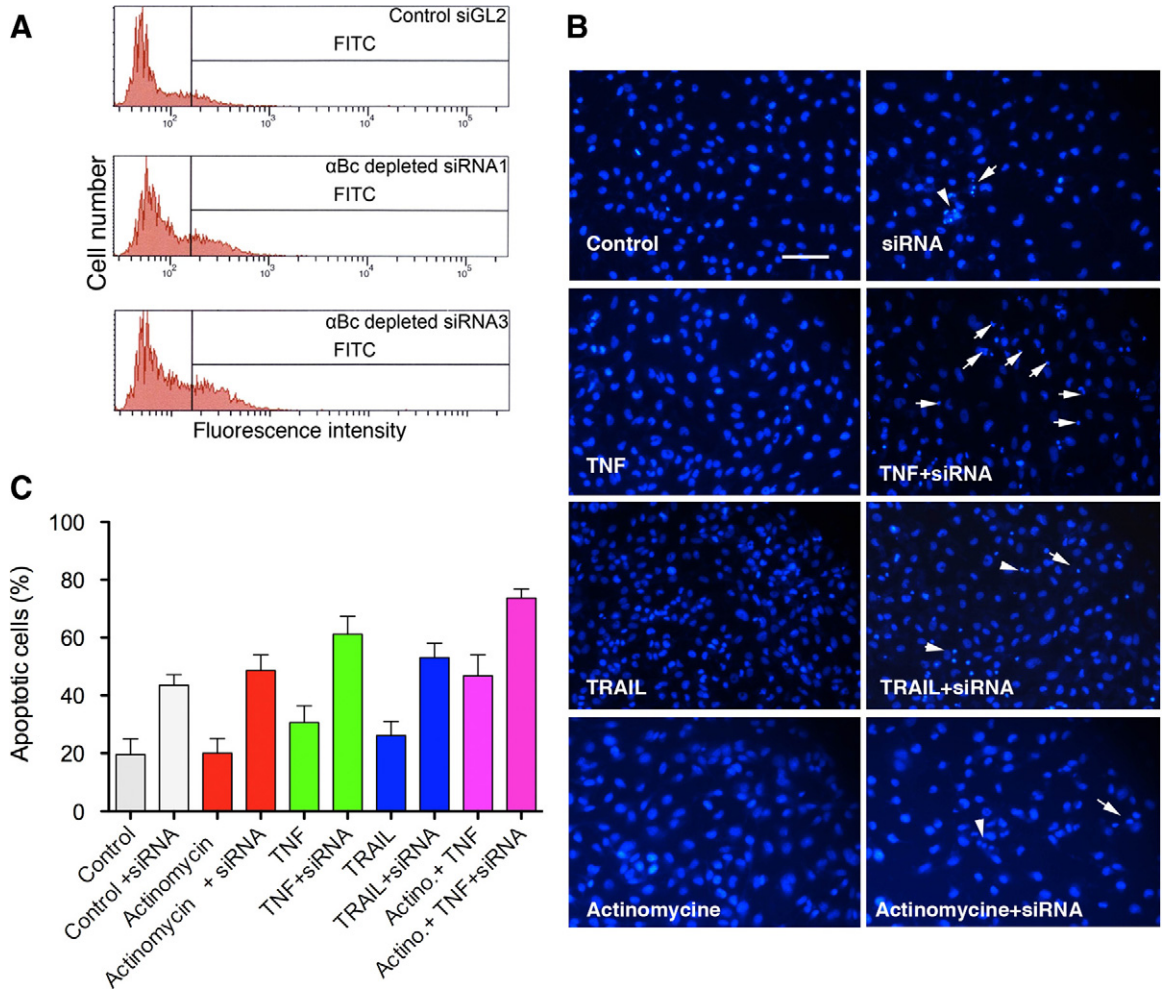

Figure 5. **A:** Antiapoptotic effects of αB-crystallin assessed by flow cytometry. **Upper:** U-373MG cells exposed to treatment with actinomycin D for 24 hours. **Middle** and **lower:** αB-crystalline-depleted U-373MG cells exposed for 24 hours to actinomycin D treatment. A higher percentage of apoptotic cells was seen in the αB-crystallin depleted cells. **B:** DAPI staining of U-373MG cells and U-373MG αBc-depleted cells treated with TNFα, TRAIL, and actinomycin D. **Arrows** point to apoptotic cells. Scale bar = 50 μm. **C:** Apoptotic cell counts revealed a significant increase in apoptotic nuclei in the cells as a function of cell treatment condition treated with siRNA, indicating that αBc has a significant role in apoptosis resistance.

In the present work we applied a new human glioma xenotransplantation model where, by serial transplantation, the phenotype changes from a highly infiltrative nonangiogenic to a less invasive highly angiogenic tumor.[9,24] This model allowed us to perform a direct comparison of differentially expressed proteins characterized by two distinct phenotypes that both show key biological features of GBMs *in situ* (ie, diffuse invasion and angiogenesis). We then used proteomics to identify proteins that characterize the two phenotypes. Even though 2D electrophoresis is limited by its detection level,[43,44] several proteins were found to be expressed at higher levels in the invasive compared to the less invasive angiogenic phenotype. Verification of the proteomics data by immunohistochemistry and Western blots confirmed that αBc was differentially expressed in invasive compared to the less invasive angiogenic tumors. By immunohistochemistry, we confirmed a strong and heterogeneous expression of αBc in human GBMs *in situ*, with unstained areas around vasculature, which is in concordance with previous data.[19] We applied tissue microarrays to assess αBc expression in low grade astrocytomas as well as in grade III anaplastic astrocytomas. Surprisingly high expression was observed in grade I and II tumors, which are characterized by a lesser aggressive clinical course than the high grade tumors. Also others have shown that αBc is expressed in low-grade astrocytomas,[19] but its exact role in these tumors is difficult to explain. Yet our data indicate that apoptosis resistance reflected by αBc overexpression is a property shared between both low- and high-grade gliomas as well as by the invasive subpopulations within the tumors. In this context it should be emphasized that low-grade tumors show extensive infiltration into the normal brain whereas predominant angiogenesis is less evident. Thus, such tumors show several growth characteristics similar to the low generation tumors observed in the present study.

Because αBc was found to be overexpressed by the invasive cells, we wanted to assess its expression in stereotactic biopsies taken from MRI-defined areas of the invasive front as well as from the tumor core. Confirming the animal observations as well as earlier data,[19] the samples obtained from the invasive tumor rim showed high expression of αBc, whereas the ones obtained from

the tumor core exhibited weaker expression (Figure 2C). Thus, these data support a potential role of αBc in the invasive cells. It should also be emphasized that also normal astrocytes may express αBc although at a lower degree, its relation to infiltration and cell migration may therefore be more a quantitative than a qualitative phenomenon.

αBc is mainly a protein localized in the cytosol and membranes/organelles fractions.[45,46] It is also present in the nucleus and mitochondria.[47–49] In the cytoplasm it is associated with cytoskeletal proteins including actin, vimentin, and desmin.[50] Moreover, αBc has together with other small heat shock proteins (HSP25 and HSP27) been shown to associate with GFAP and protect astrocytes against stress by proteasomal inhibition.[15–17,51] To show an association between αBc and migrating glioma cells, we knocked down αBc in both low-generation biopsy spheroids as well as in cell lines showing endogenous expression of αBc. Both experiments show a reduced number of migrating cells after αBc depletion. We then overexpressed αBc in U87 cells and performed migration and proliferation assays. Interestingly, the U87αBC cells did not show any increase in migration and proliferation (Figure 4), indicating that αBc is not directly linked to cell migration. At present there is an increasing body of evidence pointing at a role of αBc in apoptosis resistance.[37–42,52] To explain the delayed wound closure and reduced spread area in the spheroid migration assay by αBc-depleted cells, we therefore hypothesized that an increased apoptosis and reduced cell number in the αBc-depleted samples was the cause of the delayed wound closure and the reduced number of cells in the migration areas (Figure 3). By depleting U-373MG for αBc we sensitized the cell to apoptosis. To assess that our findings were not a cell line specific phenomenon related to U-373MG we also performed similar experiments using U251 cells and got similar results (data not shown). Recent studies indicate that invasive glioma cells are resistant to apoptosis and that apoptosis is suppressed when cells adopt a migratory phenotype.[53,54] Using cDNA microarrays, Mariani et al showed that invasive glioma cells display a shift in expression of apoptosis regulatory genes favoring decreased ability to undergo apoptosis.[33] Also, overexpression of the survival enhancer Bcl-2 promotes glioma cell invasion.[55] On the other hand the expression of promigratory scatter factor/hepatocyte growth factor inhibits apoptosis of migrating GBM cells.[56]

In conclusion, αBc is more strongly expressed by GBM cells that infiltrate the brain where it exerts its main biological action by preventing apoptosis. In our view, αBc should be further exploited as a therapeutic target toward invasive glioma cells.

Acknowledgments

We thank Erna Finsås, Tove Johansen, and Vanessa Barthelemy for technical assistance and Lene Nybø for animal care. We thank our colleagues at PROBE (*http://www.probe.uib.no*) for all of the help and expertise in performing mass spectrometry. We also thank Hege Avaldsnes Dale and Endy Spriet at MIC (Molecular Imaging Center) for the assistance in obtaining the confocal microscope images. We acknowledge Petr Nazarov for help with the statistical analysis.

References

1. Norden AD, Wen PY: Glioma therapy in adults. Neurologist 2006, 12:279–292
2. Giese A, Westphal M: Glioma invasion in the central nervous system. Neurosurgery 1996, 39:235–250; discussion 250–232
3. Giese A, Bjerkvig R, Berens ME, Westphal M: Cost of migration: invasion of malignant gliomas and implications for treatment. J Clin Oncol 2003, 21:1624–1636
4. Rempel SA, Ge S, Gutierrez JA: SPARC: a potential diagnostic marker of invasive meningiomas. Clin Cancer Res 1999, 5:237–241
5. Tysnes BB, Mahesparan R: Biological mechanisms of glioma invasion and potential therapeutic targets. J Neurooncol 2001, 53:129–147
6. Gunther W, Skaftnesmo KO, Arnold H, Terzis AJ: Molecular approaches to brain tumour invasion. Acta Neurochir (Wien) 2003, 145:1029–1036
7. Bjerkvig R, Tonnesen A, Laerum OD, Backlund EO: Multicellular tumor spheroids from human gliomas maintained in organ culture. J Neurosurg 1990, 72:463–475
8. Engebraaten O, Bjerkvig R, Lund-Johansen M, Wester K, Pedersen PH, Mork S, Backlund EO, Laerum OD: Interaction between human brain tumour biopsies and fetal rat brain tissue in vitro. Acta Neuropathol (Berl) 1990, 81:130–140
9. Sakariassen PO, Prestegarden L, Wang J, Skaftnesmo KO, Mahesparan R, Molthoff C, Sminia P, Sundlisaeter E, Misra A, Tysnes BB, Chekenya M, Peters H, Lende G, Kalland KH, Oyan AM, Petersen K, Jonassen I, van der Kogel A, Feuerstein BG, Terzis AJ, Bjerkvig R, Enger PO: Angiogenesis-independent tumor growth mediated by stem-like cancer cells. Proc Natl Acad Sci USA 2006, 103:16466–16471
10. Klemenz R, Frohli E, Steiger RH, Schafer R, Aoyama A: Alpha B-crystallin is a small heat shock protein. Proc Natl Acad Sci USA 1991, 88:3652–3656
11. Aoyama A, Frohli E, Schafer R, Klemenz R: Alpha B-crystallin expression in mouse NIH 3T3 fibroblasts: glucocorticoid responsiveness and involvement in thermal protection. Mol Cell Biol 1993, 13:1824–1835
12. Horwitz J: Alpha-crystallin can function as a molecular chaperone. Proc Natl Acad Sci USA 1992, 89:10449–10453
13. Kantorow M, Piatigorsky J: Alpha-crystallin/small heat shock protein has autokinase activity. Proc Natl Acad Sci USA 1994, 91:3112–3116
14. Iwaki T, Wisniewski T, Iwaki A, Corbin E, Tomokane N, Tateishi J, Goldman JE: Accumulation of alpha B-crystallin in central nervous system glia and neurons in pathologic conditions. Am J Pathol 1992, 140:345–356
15. Nicholl ID, Quinlan RA: Chaperone activity of alpha-crystallins modulates intermediate filament assembly. EMBO J 1994, 13:945–953
16. Perng MD, Cairns L, van den IP, Prescott A, Hutcheson AM, Quinlan RA: Intermediate filament interactions can be altered by HSP27 and alphaB-crystallin. J Cell Sci 1999, 112:2099–2112
17. Wisniewski T, Goldman JE: Alpha B-crystallin is associated with intermediate filaments in astrocytoma cells. Neurochem Res 1998, 23:385–392
18. Iwaki T, Iwaki A, Miyazono M, Goldman JE: Preferential expression of alpha B-crystallin in astrocytic elements of neuroectodermal tumors. Cancer 1991, 68:2230–2240
19. Hitotsumatsu T, Iwaki T, Fukui M, Tateishi J: Distinctive immunohistochemical profiles of small heat shock proteins (heat shock protein 27 and alpha B-crystallin) in human brain tumors. Cancer 1996, 77:352–361
20. de Ridder LI, Laerum OD, Mork SJ, Bigner DD: Invasiveness of human glioma cell lines in vitro: relation to tumorigenicity in athymic mice. Acta Neuropathol (Berl) 1987, 72:207–213
21. Engebraaten O, Hjortland GO, Hirschberg H, Fodstad O: Growth of precultured human glioma specimens in nude rat brain. J Neurosurg 1999, 90:125–132
22. Thorsen F, Ersland L, Nordli H, Enger PO, Huszthy PC, Lundervold A,

Standnes T, Bjerkvig R, Lund-Johansen M: Imaging of experimental rat gliomas using a clinical MR scanner. J Neurooncol 2003, 63:225–231
23. Enger PO, Thorsen F, Lonning PE, Bjerkvig R, Hoover F: Adeno-associated viral vectors penetrate human solid tumor tissue in vivo more effectively than adenoviral vectors. Hum Gene Ther 2002, 13:1115–1125
24. Goplen D, Wang J, Enger PO, Tysnes BB, Terzis AJ, Laerum OD, Bjerkvig R: Protein disulfide isomerase expression is related to the invasive properties of malignant glioma. Cancer Res 2006, 66:9895–9902
25. Balgley BM, Laudeman T, Yang L, Song T, Lee CS: Comparative evaluation of tandem MS search algorithms using a target-decoy search strategy. Mol Cell Proteomics 2007, 6:1599–1608
26. Voges J, Schroder R, Treuer H, Pastyr O, Schlegel W, Lorenz WJ, Sturm V: CT-guided and computer assisted stereotactic biopsy. Technique, results, indications. Acta Neurochir (Wien) 1993, 125:142–149
27. Jul-Larsen A, Visted T, Karlsen BO, Rinaldo CH, Bjerkvig R, Lonning PE, Boe SO: PML-nuclear bodies accumulate DNA in response to polyomavirus BK and simian virus 40 replication. Exp Cell Res 2004, 298:58–73
28. Ruitenberg MJ, Plant GW, Christensen CL, Blits B, Niclou SP, Harvey AR, Boer GJ, Verhaagen J: Viral vector-mediated gene expression in olfactory ensheathing glia implants in the lesioned rat spinal cord. Gene Ther 2002, 9:135–146
29. Lefranc F, Brotchi J, Kiss R: Possible future issues in the treatment of glioblastomas: special emphasis on cell migration and the resistance of migrating glioblastoma cells to apoptosis. J Clin Oncol 2005, 23:2411–2422
30. Uhm JH, Dooley NP, Kyritsis AP, Rao JS, Gladson CL: Vitronectin, a glioma-derived extracellular matrix protein, protects tumor cells from apoptotic death. Clin Cancer Res 1999, 5:1587–1594
31. Aoyama A, Steiger RH, Frohli E, Schafer R, von Deimling A, Wiestler OD, Klemenz R: Expression of alpha B-crystallin in human brain tumors. Int J Cancer 1993, 55:760–764
32. Odreman F, Vindigni M, Gonzales ML, Niccolini B, Candiano G, Zanotti B, Skrap M, Pizzolitto S, Stanta G, Vindigni A: Proteomic studies on low- and high-grade human brain astrocytomas. J Proteome Res 2005, 4:698–708
33. Mariani L, Beaudry C, McDonough WS, Hoelzinger DB, Demuth T, Ross KR, Berens T, Coons SW, Watts G, Trent JM, Wei JS, Giese A, Berens ME: Glioma cell motility is associated with reduced transcription of proapoptotic and proliferation genes: a cDNA microarray analysis. J Neurooncol 2001, 53:161–176
34. Chelouche-Lev D, Kluger HM, Berger AJ, Rimm DL, Price JE: alphaB-crystallin as a marker of lymph node involvement in breast carcinoma. Cancer 2004, 100:2543–2548
35. Moyano JV, Evans JR, Chen F, Lu M, Werner ME, Yehiely F, Diaz LK, Turbin D, Karaca G, Wiley E, Nielsen TO, Perou CM, Cryns VL: AlphaB-crystallin is a novel oncoprotein that predicts poor clinical outcome in breast cancer. J Clin Invest 2006, 116:261–270
36. Cicek M, Samant RS, Kinter M, Welch DR, Casey G: Identification of metastasis-associated proteins through protein analysis of metastatic MDA-MB-435 and metastasis-suppressed BRMS1 transfected-MDA-MB-435 cells. Clin Exp Metastasis 2004, 21:149–157
37. Gruvberger-Saal SK, Parsons R: Is the small heat shock protein alphaB-crystallin an oncogene?. J Clin Invest 2006, 116:30–32
38. Kamradt MC, Chen F, Cryns VL: The small heat shock protein alpha B-crystallin negatively regulates cytochrome c- and caspase-8-dependent activation of caspase-3 by inhibiting its autoproteolytic maturation. J Biol Chem 2001, 276:16059–16063
39. Liu B, Bhat M, Nagaraj RH: AlphaB-crystallin inhibits glucose-induced apoptosis in vascular endothelial cells. Biochem Biophys Res Commun 2004, 321:254–258
40. Kamradt MC, Lu M, Werner ME, Kwan T, Chen F, Strohecker A, Oshita S, Wilkinson JC, Yu C, Oliver PG, Duckett CS, Buchsbaum DJ, LoBuglio AF, Jordan VC, Cryns VL: The small heat shock protein alpha B-crystallin is a novel inhibitor of TRAIL-induced apoptosis that suppresses the activation of caspase-3. J Biol Chem 2005, 280:11059–11066
41. Stegh AH, Chin L, Louis DN, DePinho RA: What drives intense apoptosis resistance and propensity for necrosis in glioblastoma? A role for Bcl2L12 as a multifunctional cell death regulator. Cell Cycle 2008, 7:2833–2839
42. Ikeda R, Yoshida K, Ushiyama M, Yamaguchi T, Iwashita K, Futagawa T, Shibayama Y, Oiso S, Takeda Y, Kariyazono H, Furukawa T, Nakamura K, Akiyama S, Inoue I, Yamada K: The small heat shock protein alphaB-crystallin inhibits differentiation-induced caspase 3 activation and myogenic differentiation. Biol Pharm Bull 2006, 29:1815–1819
43. Wilkins MR, Gasteiger E, Sanchez JC, Bairoch A, Hochstrasser DF: Two-dimensional gel electrophoresis for proteome projects: the effects of protein hydrophobicity and copy number. Electrophoresis 1998, 19:1501–1505
44. Chambers G, Lawrie L, Cash P, Murray GI: Proteomics: a new approach to the study of disease. J Pathol 2000, 192:280–288
45. Simon S, Fontaine JM, Martin JL, Sun X, Hoppe AD, Welsh MJ, Benndorf R, Vicart P: Myopathy-associated alphaB-crystallin mutants: abnormal phosphorylation, intracellular location, and interactions with other small heat shock proteins. J Biol Chem 2007, 282:34276–34287
46. Sun Y, MacRae TH: Small heat shock proteins: molecular structure and chaperone function. Cell Mol Life Sci 2005, 62:2460–2476
47. Gangalum RK, Schibler MJ, Bhat SP: Small heat shock protein alphaB-crystallin is part of cell cycle-dependent Golgi reorganization. J Biol Chem 2004, 279:43374–43377
48. Bhat SP, Hale IL, Matsumoto B, Elghanayan D: Ectopic expression of alpha B-crystallin in Chinese hamster ovary cells suggests a nuclear role for this protein. Eur J Cell Biol 1999, 78:143–150
49. van Rijk AE, Stege GJ, Bennink EJ, May A, Bloemendal H: Nuclear staining for the small heat shock protein alphaB-crystallin colocalizes with splicing factor SC35. Eur J Cell Biol 2003, 82:361–368
50. Maddala R, Rao VP: alpha-Crystallin localizes to the leading edges of migrating lens epithelial cells. Exp Cell Res 2005, 306:203–215
51. Goldbaum O, Riedel M, Stahnke T, Richter-Landsberg C: The small heat shock protein HSP25 protects astrocytes against stress induced by proteasomal inhibition. Glia 2009, 57:1566–1577
52. Stegh AH, Kesari S, Mahoney JE, Jenq HT, Forloney KL, Protopopov A, Louis DN, Chin L, DePinho RA: Bcl2L12-mediated inhibition of effector caspase-3 and caspase-7 via distinct mechanisms in glioblastoma. Proc Natl Acad Sci USA 2008, 105:10703–10708
53. Schauff AK, Kim EL, Leppert J, Nadrowitz R, Wuestenberg R, Brockmann MA, Giese A: Inhibition of invasion-associated thromboxane synthase sensitizes experimental gliomas to gamma-radiation, J Neurooncol 2009, 91:241–249
54. Nakada M, Nakada S, Demuth T, Tran NL, Hoelzinger DB, Berens ME: Molecular targets of glioma invasion. Cell Mol Life Sci 2007, 64:458–478
55. Wick W, Wagner S, Kerkau S, Dichgans J, Tonn JC, Weller M: BCL-2 promotes migration and invasiveness of human glioma cells. FEBS Lett 1998, 440:419–424
56. Bowers DC, Fan S, Walter KA, Abounader R, Williams JA, Rosen EM, Laterra J: Scatter factor/hepatocyte growth factor protects against cytotoxic death in human glioblastoma via phosphatidylinositol 3-kinase- and AKT-dependent pathways. Cancer Res 2000, 60:4277–4283